Environ Geochem Health (2021) 43:1891–1902
https://doi.org/10.1007/s10653-020-00768-z

ORIGINAL PAPER

Oyster shell powder for Pb(II) immobilization in both aquatic and sediment environments

Gansheng Zhong · Yunsong Liu · Yuanyuan Tang

Received: 27 June 2020 / Accepted: 30 October 2020 / Published online: 11 November 2020

Abstract Heavy metal pollution has always been a serious environmental problem widely concerned by researchers all around the world. On the other side, the accumulation of biowastes has also occupied a large amount of space and caused a series of environment pollution. In this study, the waste oyster shell, was applied as a type of biogenic carbonate material for Pb(II) removal from the aquatic environment, and further as a remediation agent for metal stabilization in the contaminated river sediment. After simple pre-treatment, the oyster shell powder (OSP) was characterized, and the results showed that the prepared OSP is mainly composed of calcite with particle size of micron-level. The OSP exhibited excellent Pb(II) adsorption performance, with the adsorption capacity as 639.9 mg/g through adsorption isotherm study. Furthermore, the OSP was applied to remediate the collected river sediment artificially contaminated by Pb(II). It was found that the proportion of residual Pb fraction (F4) was greatly increased from 39.6% of the original sediment to 76.7% in the 14-day incubated sediment with OSP. The Pb(II) concentration after leaching procedure was decreased from 810.7 to 108.6 μg/L even after 5-day incubation. Therefore, this study shows the potential of using waste oyster shell as adsorbent and amendment agent for effective metal immobilization in both aquatic and sediment systems.

Electronic supplementary material The online version of this article (https://doi.org/10.1007/s10653-020-00768-z) contains supplementary material, which is available to authorized users.

G. Zhong · Y. Liu · Y. Tang (✉)
Guangdong Provincial Key Laboratory of Soil and Groundwater Pollution Control, School of Environmental Science and Engineering, Southern University of Science and Technology, Shenzhen 518055, China
e-mail: tangyy@sustech.edu.cn

G. Zhong · Y. Liu · Y. Tang
State Environmental Protection Key Laboratory of Integrated Surface Water-Groundwater Pollution Control, School of Environmental Science and Engineering, Southern University of Science and Technology, Shenzhen 518055, China

Y. Liu
School of Urban Planning and Design, Peking University Shenzhen Graduate School, Nanshan District, Shenzhen 518055, China

Graphic abstract

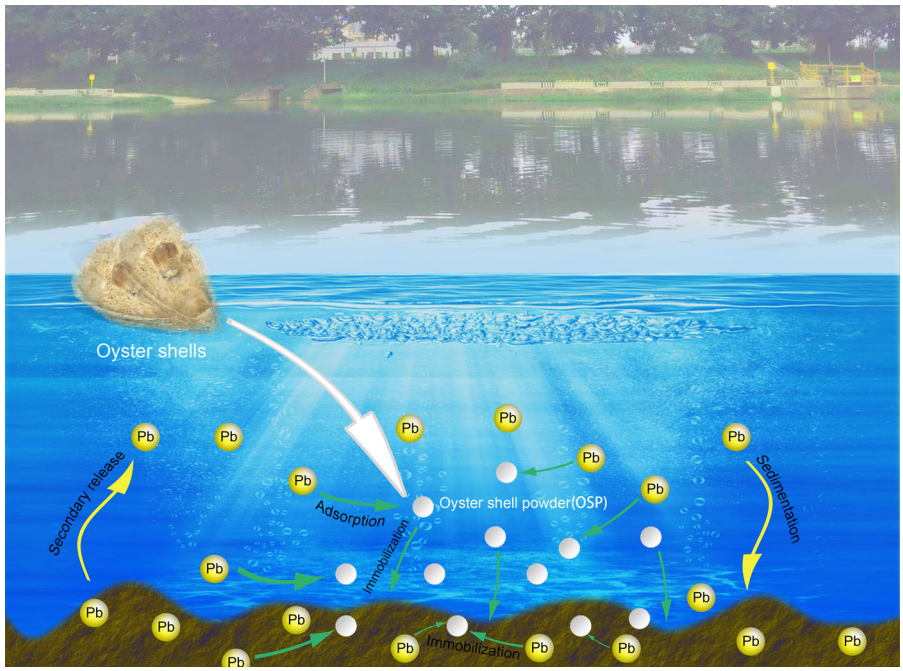

Keywords Oyster shell powder · Lead · Adsorption · Aquatic environment · Stabilization · Sediment

Introduction

Heavy metals with high mobility from industrial activities like mineral excavation, metallurgy and battery manufacturing, have been quickly transferring into the sediments of urban rivers and lakes (Dai et al. 2018). As the transportation sink of environmental pollutants, sediment can also become the source of heavy metals pollution (Ip et al. 2007; Che et al. 2003; Audry et al. 2004). For example, under certain conditions, the amount of heavy metals in sediment accounts for 99% of those of the water ecosystem (Peng et al. 2018). Once the physicochemical properties of the sediment change, heavy metals in sediments will be back into rivers in strong migratory form by the processes of desorption, dissolution, oxidation or reduction, leading secondary pollution in water body (Fonti et al. 2015). For this reason, heavy metal contaminated sediments will increase the probability of the situation that people are exposed to the environment with high concentrations of heavy metals. Therefore, the treatment and control of heavy metals in sediments should be of great significance.

To control the secondary pollution caused by heavy metal release from the sediments, remediation methods tailored to the polluted sediments include physical, chemical, biological, and the combined methods. These methods above can relive the secondary metal pollution from the sediments from three aspects including eliminating or decreasing the toxicity of heavy metals, transforming contaminated sediments to harmless materials, or separating the contaminated sediments from water ecosystem (Zhang et al. 2019a; Liu et al. 2019a). Stabilization/solidification (S/S) is one commonly used method to reduce the mobility of harmful metals by adding the remediation agents into the sediment. The application of the agents can further prevent the release of heavy metals by the way of changing the metal speciation in contaminated

sediments into low mobility and innoxious state (Cerbo et al. 2017; Xia et al. 2017). Time saving and cost-efficient are attractive advantages of S/S remediation for contaminated sediments (Wang et al. 2019; Rađenović et al. 2019). Common reagents for S/S are usually synthesized chemicals like phosphates, silico-calcium materials, and iron-bearing materials (Peng et al. 2018). Comparing with the synthesized materials above, the application of biogenic materials has become increasingly attractive due to its abundant and environmentally friendly feature.

$CaCO_3$ is one of the most commonly used materials for sediment remediation due to its high performance and low cost (Islam et al. 2017a; Jacob et al. 2018), but the $CaCO_3$ is mostly harvested by geological mining which may cause damage to the surrounding environment. In this case, some recent studies have started to obtain the $CaCO_3$ from a variety of biological products like marine shells, eggshells, sepia, etc. (Ok et al. 2011a; Guru and Dash 2014; Lim et al. 2016). The application of the biogenic carbonate materials for the heavy metal removal and stabilization has been reported in recent years. For example, the biogenic aragonite and calcined mollusk shells were used as effective adsorbents to remove Pb, Zn and Cd from the polluted water (Du et al. 2011; Köhler et al. 2007). Studies have also been conducted on using calcined cockle shells to stabilize heavy metals in soil, which reduced the leaching of Pb, Cd and Zn by 85%, 85%, 91%, respectively (Islam et al. 2017b). The oyster shells have also been found with strong abilities for heavy metal adsorption due to the presence of calcium carbonate layer structures including prismatic part and nacreous part (Wu et al. 2014). Therefore, with characteristic structures, it is assumed that the oyster shells can become a high-quality substitute for mineral calcium carbonate. However, the oyster shells have been regarded as solid wastes and finally go to landfilling (Alvarenga et al. 2012), which cause a great waste of $CaCO_3$ materials together with a serious burden for solid waste management. Nowadays, there are some recent studies using the oyster shell powder for wastewater treatment and soil remediation (Zhang et al. 2019b; Moon et al. 2011; Jung et al. 2016), which inspired their potential utilization for heavy metal immobilization in the river sediments. Moreover, the aquatic environment above the sediment is an inextricable part of the river system. Therefore, the application of the oyster shell powder for metal adsorption in aquatic environment as well as metal stabilization in sediment is equally important, and can meet the practical requirement for the remediation of real river system. Investigating the adsorption performance of the amendment agent can evaluate the interaction between metal ions and the adsorbent, and further estimate the possibility of secondary metal release after metal remediation. In addition, lead is one commonly detected heavy metal in the sediment, which may cause remarkable inhibiting effect on aquatic plants and increasing pathogenic possibility of human.

Therefore, in this study, we applied the waste oyster shell powder for lead adsorption in solution, and then further adopted this material for lead stabilization in the contaminated sediment. During this study, the lead adsorption behavior of oyster shell powder was examined, including adsorption kinetics, isotherm, as well as the effect of factors like pH, solid-to-liquid ratio and initial lead concentration. Moreover, the lead stabilization performance was evaluated after adding the shell powder as remediation agent in the sediment.

Materials and methods

Sample preparation

The oyster shells were purchased from an aquarium store collecting abandoned oyster shells as filter material in Guangdong province. The powder sample from the purchased oyster shells was prepared according to the following procedures. The original shells were washed by water and then dried naturally. After that, the shells were broken into small lumps, ground into powder and then sieved through a 100-mesh sieve. Finally, the fine powder after sieving was then ball-milled for four times, with 5 min at each time. The residual powder sample were then mixed uniformly and stored until use, which was denoted as OSP (oyster shell powder) hereafter.

The sediments for experiment were collected randomly at subsurface 0–20 cm from the downstream of Maozhou river in October 2018 (geographical coordinates: 113.829°E, 22.791°N) (Liu et al. 2019b). The collected sediments were well mixed, dried, milled and finally passed through a 100-mesh sieve. The pH and moisture content of sediments were tested according to procedures as below: 0.5 g of air-dried

sediment was added into 25 mL ultrapure water. After agitated for 24 h, the pH value of the solution mixture was measured. The moisture content was measured according to the weight loss of the sediment after drying at 105 °C. Moreover, the Pb-enriched sediment was particularly prepared for the stabilization of Pb in the sediment after adding OSP. For which, 10 g of the dry sediment was added into a beaker containing 100 mL ultrapure water with 24 mg $Pb(NO_3)_2$. The turbid liquid was stirred with a magnetic stirrer for 12 h to obtain a sufficiently uniform sediment sample enriched by Pb. Then, the liquid content in the mixture was evaporated at 60 °C in an oven. After procedures above, the pH value of the raw sediment is within the range of 5.95–6.06, while the water content is 60.19%. After Pb enrichment, the Pb content in the sediment was measured as 1536.9 mg/kg.

Characterization

The phase composition of the samples was detected by an X-ray powder diffractometer (XRD, Smartlab, Japan) with Cu−Kα radiation. Diffraction patterns were collected over $2\theta = 10°-90°$ at 10°/min. The micro-morphology of the OSP was observed by conducting a scanning electron microscopy analysis (SEM, Merlin, Germany) with different magnification times. A thermogravimetric and differential thermal analyzer (TG–DTA. Hengjiu HCT-1, China) was used to conduct a thermogravimetric and differential thermal analysis of OSP to get the weight loss and differential quantity of heat during combustion. The DTA data was compared to that of other researches that mentioned oyster shell powder or other biological calcium carbonates. The particle size of the OSP was detected by a nanoparticle size and zeta point analyzer (Malvern, UK). The multipoint Brunauer−Emmett−Teller (BET, Micromeritics ASAP 2460, USA) method was adopted to obtain the surface areas of the solid samples.

Pb(II) adsorption in aqueous solution

Pb(II) solution for adsorption experiments was prepared by mixing $Pb(NO_3)_2$ (AR, Fuchen, China) with deionized water at a certain ratio. The volume of all solutions were fixed at 50 mL with a temperature of 25 °C. The pH effect on Pb adsorption was analyzed by changing pH from 3.0 to 6.0 for 4 h. However, as shown in Figure S1, the adsorption efficiency were all calculated as $\sim$ 100% in solutions with initial Pb(II) concentration of 700 mg/L at different pH value. The results indicate that pH value is not a key factor, and thus pH 5.0 was selected for further experiments. The dosage of OSP for Pb adsorption was set as 0.01 g, 0.02 g, 0.05 g, 0.1 g, 0.2 g, 0.5 g for 50 mL of the Pb(II) solution (700 mg/L). After that, the mixture of OSP and Pb(II) solution was kept stirring until finishing the experiment. All adsorption experiments were conducted in triplicate. The Pb(II) concentration in any solution was tested by an inductively coupled plasma optical emission spectrometer (ICP-OES, Optima8000, PerkinElmer). The Pb(II) adsorption capacity (q_e) of the OSP was calculated according to Eq. 1 as follows:

$$q_e = \frac{(C_0 - C_e) * V}{m} \tag{1}$$

where q_e (mg/g) is the adsorption capacity of the OSP at equilibrium, m is the weight of the OSP (g), V is the volume of the solution, while C_0 and C_e (mg/L) refer to the initial and equilibrium Pb(II) concentration, respectively.

For adsorption kinetics analysis, a fixed volume of solution (10 mL) was taken out at time intervals of 0, 5, 10, 15, 30, 45, 60, 90, 120, 180, 240 min. The samples were passed through 0.45 μm membrane and the concentrations of Pb(II) were analyzed by ICP-OES. Then, the adsorption capacities calculated from equilibrium Pb(II) concentrations at different contact time were fitted to the pseudo-first-order model and pseudo-second-order model as follows (Eqs. 2 and 3):

Pseudo-first-order model:

$$\log(q_e - q) = \log q_e - \frac{k_1 t}{2.303} \tag{2}$$

Pseudo-second-order model:

$$\frac{t}{q} = \frac{1}{k_2 q_e^2} + \frac{t}{q_e} \tag{3}$$

where k_1 (min^{-1}) is the pseudo-first order rate constant. q_e and q (mg/g) are the adsorption amount at equilibrium and time t, respectively.

For adsorption isotherm, the initial Pb(II) concentrations was set as 100, 300, 500, 700, 900, 1100 mg/L for 3 h adsorption with OSP dosage of 1 g/L. Two

equilibrium models, Langmuir and Freundlich isotherm equations, were adopted for the isotherm analysis, with linear formulas as followings (Eqs. 4 and 5):

Langmuir model:

$$\frac{C_e}{q_e} = \frac{1}{K_L q_{\max}} + \frac{C_e}{q_{\max}} \quad (4)$$

Freundlich model:

$$\ln q_e = \ln K_F + \frac{1}{n}\ln C_e \quad (5)$$

where C_e (mg/L) is the Pb(II) concentration at equilibrium and q_e (mg/g) refers to the adsorption capacity. $q_{\max}$ (mg/g) is the maximum adsorption capacity. K_L is Langmuir constant while K_F and n are Freundlich constants.

Experiments for Pb(II) stabilization in the amended sediment

0.2 g of the OSP was added in 1 g of the pretreated sediment. The incubation time (5 and 14 days) was selected to examine the stabilization of Pb(II) in the sediment. The mixtures were centrifuged at 3000 rpm after incubation in dark environment, and then the solid samples were further dried for further experiments. The blank experiments were also conducted for the sediments without OSP. The speciation of Pb in the amended sediment was analyzed by the modified BCR sequential extraction with details provided in the Supporting Information (Sect. 2). Generally speaking, the metal speciation can be divided into four different fractions, including exchangeable metal and carbonate-associated fraction (F1), fraction associated with Fe–Mn oxides (F2), fraction bound to organic matter (F3), and residual fraction (F4). But we also measured the Pb(II) content in the supernatant marked as Fraction 0 (F0) but under detection limit.

Toxicity characteristic leaching procedure

The toxicity characteristic leaching procedure (TCLP) was also carried out to evaluate the leachability of Pb after sediment remediation. The raw sediment and the samples after incubation were all tested according to the standard TCLP procedure. 0.5 g solid sample was put in a centrifuge tube with 10 mL acetic acid (0.1 mol/L pH = 2.88 ± 0.05). Then the centrifuge tubes were rotated at a speed of 30 r/min for 18 h, and the supernatant was obtained afterwards by centrifuging the mixture after leaching at a speed of 4000 r/min. After that, the supernatant was further filtered by 0.45 μm membrane filter with a syringe, and the Pb concentration was detected by an inductively coupled plasma-mass spectrometry (ICP-MS, 7700, Agilent Technologies, USA).

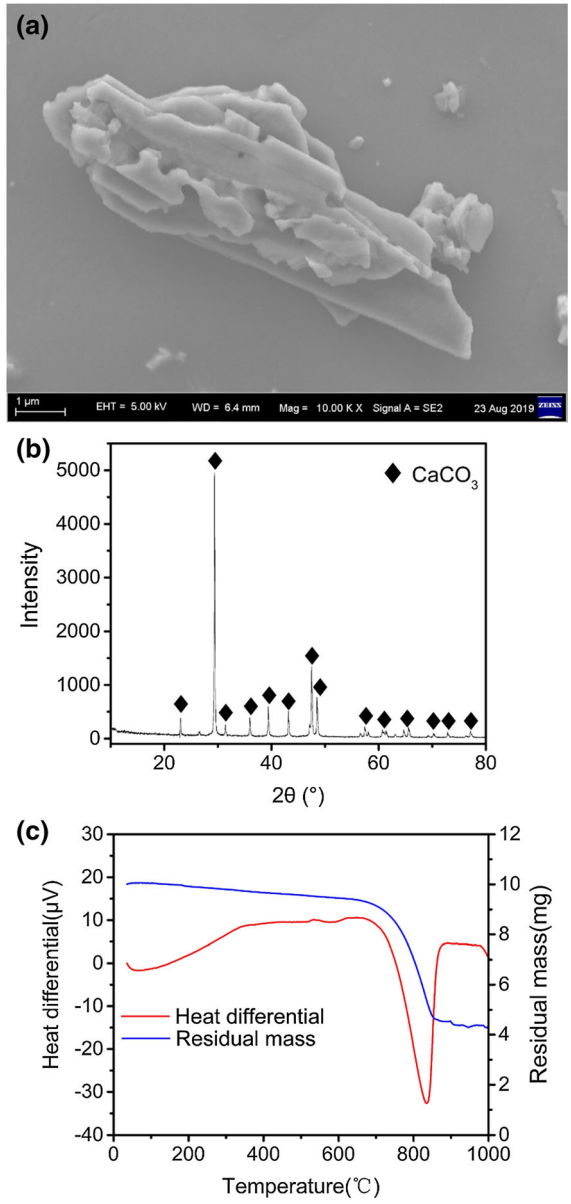

Fig. 1 **a** SEM image, **b** XRD pattern, and **c** TG curve (blue) and DTA curve (red) of the oyster shell powder (OSP) after pretreatment

Results and discussion

Characterizations of oyster shell powder

The microstructure of OSP after ball grinding was observed by SEM (Fig. 1a), which shows that the OSP were crushed into particles with different layers. Besides that, some small single-layer pieces were also observed and adhered on the larger particles. The particle size of the OSP was analyzed with an averaged particle diameter (Z-Average) as 1062.5 nm. The crystal structure of the OSP sample was shown by the XRD pattern as shown in Fig. 1b, which is consistent with the standard pattern of calcium carbonate (calcite, PDF#99-0022). The high and sharp peaks in the XRD pattern illustrate the purity of OSP with well crystalized calcite. TG–DTA analysis was further conducted on the OSP, with results shown in Fig. 1c. The mass of the OSP was decreased significantly when the heating temperature reached 700 °C, and finally stabilized at 800 °C where about 45% of the original mass was left. Similar results were reported by other researchers (Jung et al. 2016; Ok et al. 2010). In addition, the specific surface area of the milled OSP was 3.869 m^2/g, in comparison with 2.438 m^2/g for the raw OSP.

Adsorption of Pb(II) in solution by oyster shell powder

Factors affecting Pb(II) adsorption

The solid-to-liquid ratio (adsorbent dosage to solution volume) has been reported as an important factor for metal adsorption. Hence, Fig. 2a summarizes the variation of Pb(II) adsorption capacity of the OSP with different solid-to-liquid ratio, which shows that the highest Pb(II) adsorption capacity (668.4 mg/g) occurred at solid-to-liquid ratio of 1 g/L. With further increase in solid-to-liquid ratio, the adsorption capacity was decreased obviously. The decrease in adsorption capacity at higher solid-to-liquid ratio is due to the unsaturated adsorption of the OSP with increased amount in the solution. Therefore, 1 g/L was selected as solid-to-liquid ratio for the subsequent adsorption experiments. The effect of contact time and initial Pb(II) concentration were also considered as key factors during the adsorption process. Figure 2b presents the changes of adsorption capacity with the variation of initial Pb(II) concentration (100, 300, 500, 700, 900, 1100 mg/L). An obvious increase in adsorption capacity was found with elevated initial Pb(II) concentration, until reaching 639.9 mg/g in the solution initially containing 1100 mg/L Pb(II) ions. With further increase in Pb(II) concentration, the growth of adsorption capacity slowed down and finally reached an equilibrium when the Pb(II) concentration is higher than 900 mg/L. As shown in Fig. 2c, the Pb(II) adsorption capacity of OSP was increased significantly during the first 120 min, and reached a value of 635.3 mg/g. Then, with prolonged time, the Pb(II) adsorption was increased slowly and finally reached equilibrium after 200 min.

Adsorption isotherm and kinetic studies

Figure 2d shows the adsorption isotherm model fitting results. According to the correlation coefficient R^2 in Table 1, the adsorption is fitted better to Langmuir adsorption model ($R^2 = 0.902$) rather than the Freundlich adsorption model ($R^2 = 0.843$), suggesting that the Pb(II) adsorption on OSP was more predominant to be monolayer adsorption than multi-layer adsorption. The Langmuir modeling is based on the adsorption on homogenous surface that is energetically and sterically independent of adsorption capacity, while the Freundlich modeling indicates the adsorption on heterogeneous surfaces (Zhou et al. 2018). Hence, the modeling results suggest that the mono-layer Pb(II) adsorption is dominant, which may be due to the reaction of $CaCO_3$ and Pb(II) ions on the sample surface. Moreover, the coefficient $1/n < 1$ ($n > 1$) means that the adsorption is a spontaneous process. Adsorption kinetics was fitted by the pseudo-first-order and pseudo-second-order models with results shown in Fig. 2e and Table 1. The R^2 value (Table 1) is 0.974 and 0.972, respectively, from the fitting results of Pb(II) adsorption by OSP to the pseudo-first-order and the pseudo-second-order models, suggesting that both physisorption and chemisorption occurred in this process (Du et al. 2011). Therefore, the chemical reaction between the Pb(II) ions and the carbonates might be intensively involved during the adsorption processes.

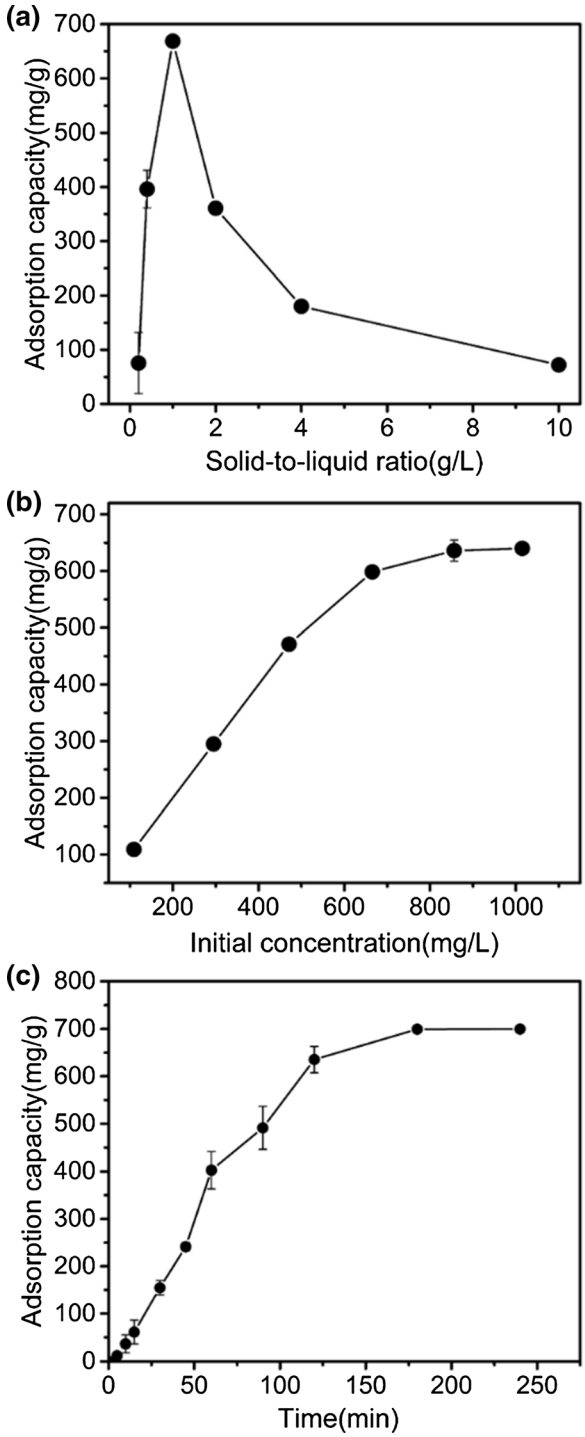

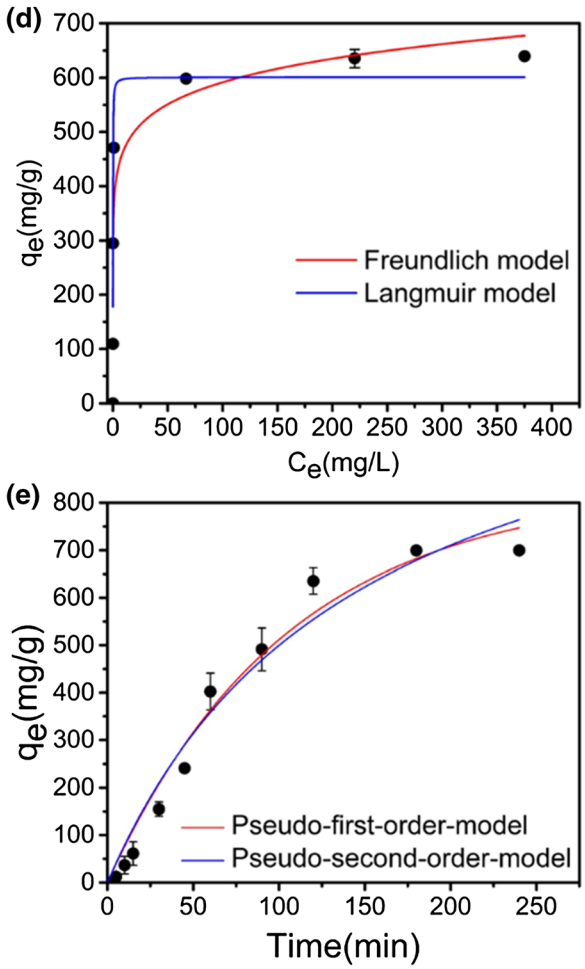

Fig. 2 Pb(II) adsorption capacity by OSP in conditions of **a** different solid-to-liquid ratio, **b** various initial Pb(II) concentration, **c** different contact time. The fitting curves of the adsorption capacity according to **d** Langmuir and Freundlich adsorption isotherms and **e** pseudo-first-order and pseudo-second-order kinetic models

Table 1 Fitting results of adsorption isotherms and kinetics

	Freundlich model			Langmuir model		
Adsorption isotherm	K_F (mg/L)	$1/n$	R^2	K_L (mg/L)	q_{max} (mg/g)	R^2
	368.93	0.1025	0.843	0.0639	601.27	0.902
	Pseudo-first-order model			Pseudo-second-order model		
Adsorption kinetic	k_1 (1/min)	q_e (mg/g)	R^2	k_2[g/(mg·min)]	q_e (mg/g)	R^2
	9.58×10^{-4}	830.15	0.974	5.58×10^{-6}	1228.51	0.972

Table 2 A comparison of Pb(II) adsorption capacity by biosource-derived adsorbents

Type of absorbent	Material	Adsorption capacity(mg/g)	References
Biochar	Cucumber skin	133.6	Basu et al. (2017)
	Ginkgo biloba	138.9	Lee et al. (2019)
	Metasequoia leaf	108.7	
	Hazelnut husk	109.9	Imamoglu et al. (2016)
Biogenic material absorbents	Egg shells	101.0	Liao et al. (2010)
	Anadara inaequivalvis shells	621.1	Bozbaş and Boz (2016)
	OSP	639.9	This study
Other absorbents	Waste polyurethane foam	14.1	Melichová and Ľuptáková (2016)
	Zeolite	43.9	
	Bentonite	48.1	

Adsorption performance and mechanisms

It can be obtained from adsorption isotherm that the maximum adsorption capacity of the OSP is 639.9 mg/g, under optimal conditions. Therefore, we briefly compare the adsorption performance among the OSP in this study and the adsorbents reported by other studies by recycling of waste resources. From the data in Table 2, generally speaking, the OSP exhibits good adsorption performance. For example, biochar is one common adsorbent derived from biowastes, and the Pb adsorption capacities of biochar were found within the range of 108.7–138.9 mg/g, which is much lower than the OSP in this study. Besides, the carbonate hydroxyapatite was extracted from the eggshell waste, and its Pb adsorption capacity is only 1/6 of the value by OSP. Moreover, *Anadara inaequivalvis* shells were also used for Pb adsorption and showed similar capacity as that of the OSP. The crystal phase of the *Anadara inaequivalvis* shells was reported as aragonite while the OSP in this study was mainly composed of calcite, resulting in a high Pb adsorption performance (Du et al. 2011).

Furthermore, the concentration of Ca in the solution after adsorption was measured and then denoted with the unit of "mmol/L" in Figure S2 of the Supporting Information, together with the amount of adsorbed Pb (mmol/L) by the OSP. From the figure, the amount of adsorbed Pb is roughly equal to that of Ca released from the OSP. Besides, a similar trend of variation was found for the concentrations of Ca and those of Pb in the solution with prolonged contact time. Therefore, it can be deduced that the major mechanism for Pb(II) adsorption is that the Ca(II) in calcium carbonate of the OSP was converted to $PbCO_3$ by ion exchange as shown in (Eq. 6). The XRD pattern was further obtained for the OSP after Pb(II) adsorption (Fig. 3a), which shows that most of the peaks were reflected from the $PbCO_3$ (PDF#99–0026, cerussite). The predominant peaks of calcite in the original OSP have been declined significantly, peak intensities of calcium carbonate, indicating that ion exchange is the critical mechanism for Pb(II) adsorption by the OSP. The

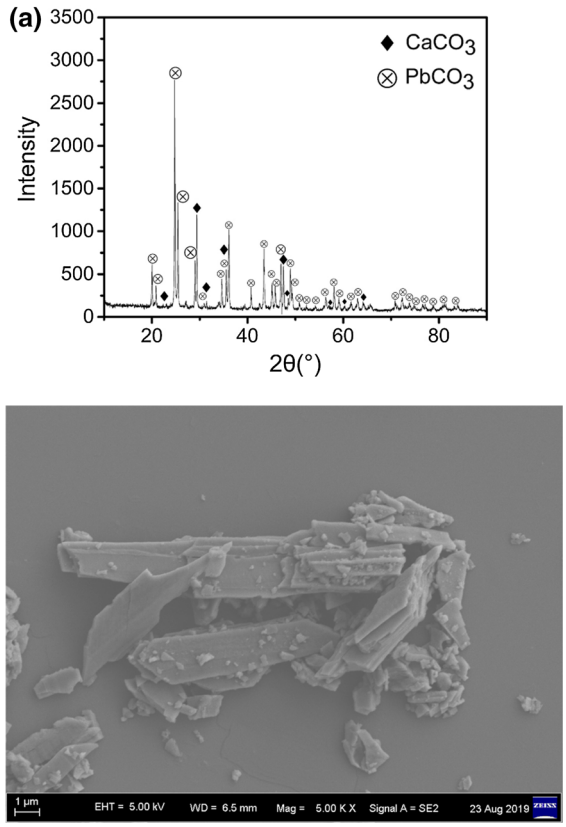

Fig. 3 **a** XRD pattern and **b** SEM image of the OSP after Pb(II) adsorption in the solution with initial Pb(II) concentration of 700 mg/g, and solid-to-liquid ratio of 1 g/L at pH = 5.0 for 2 h

SEM image of the OSP after Pb(II) adsorption is further demonstrated in Fig. 3b, with obvious particles attached on the OSP, probably as the precipitation of $PbCO_3$ after ion exchange. The combination of Pb(II) with CO_3^{2-} of the calcium carbonates has also been reported in other studies (Hu et al. 2019).

$$CaCO_3 + Pb^{2+} \rightarrow Ca^{2+} + PbCO_3 \quad (6)$$

Pb stabilization in sediment amended by oyster shell powder

The prepared OSP was added in the Pb-enriched sediment as amendments for metal solidification/stabilization. Before data analysis of the four-step BCR sequential extraction, the total amount of lead before and after the extraction were compared to evaluate the recovery rate of the metal. The sum of Pb content in the all BCR fractions (F0 + F1 + F2 + F3 + F4) was divided by the total amount of heavy metals in the original sediment, and such proportion was named as recovery rate (%). The recovery rate within 90–110% indicates reliable and referable BCR extraction. In this study, the recovery rates of original sediments and remediation experiments were calculated within the range of 90.4–105.4%, meeting the standard of recovery rate.

The percentage of different fractions of the Pb speciation (F1–F4) is illustrated in Fig. 4a. The F1 value was very small with neglectable changes for the all experimental groups. The percentage of F2 accounts for relatively high proportion for the original Pb-enriched sediment with the value of 40.1%, and such value was found as 35.9% and 31.6% for the blank samples after 5 and 14 days incubation, respectively. However, after adding the OSP, the F2 percentage was decreased substantially from 40.2% in original sediment to 3.7% and 2.8% with the incubation time as 5 and 14 days, respectively. Meanwhile, the percentage of F3 in the original Pb-enriched sediment was 18.6% and varied slightly for the blank samples after incubation (15.8% and 16.6%). However, the F3 value of the amended sediment was found as 31.8% and 20.3% after being included for 5 and 14 days, respectively. Moreover, as the most stable fraction, F4 occupied 36.9% in the original Pb-enriched sediment, and changed to 47.5% and 50.4% after incubation. While for the OSP-amended samples, the F4 fraction was found as 63.1% in 5 day-incubated sediment and further increased to 76.7% after 14 day incubation. Results show that the substantial decrease in F2 fraction after remediation is due to transformation of Pb speciation to F3 and F4 fractions. With prolonged incubation time, the F3 speciation was further transformed into the F4 fraction, which can be verified from the increase in F4 fraction after 14 day's incubation. Moreover, the exact amount of different fractions is further summarized in Table S1 of the Supporting Information, which shows that adding OSP as the amendment has significantly increased the residual fraction of Pb from 642.5 mg/kg in the original sample to 899.4 mg/kg and 1229.7 mg/kg after incubating for 5 and 14 days, respectively.

The concentrations of Pb(II) after TCLP leaching were further measured in the leachates of blank samples and amended sediments, with results shown in Fig. 4b. For the blank and amended sediments after 5 days incubation, the Pb concentration in the

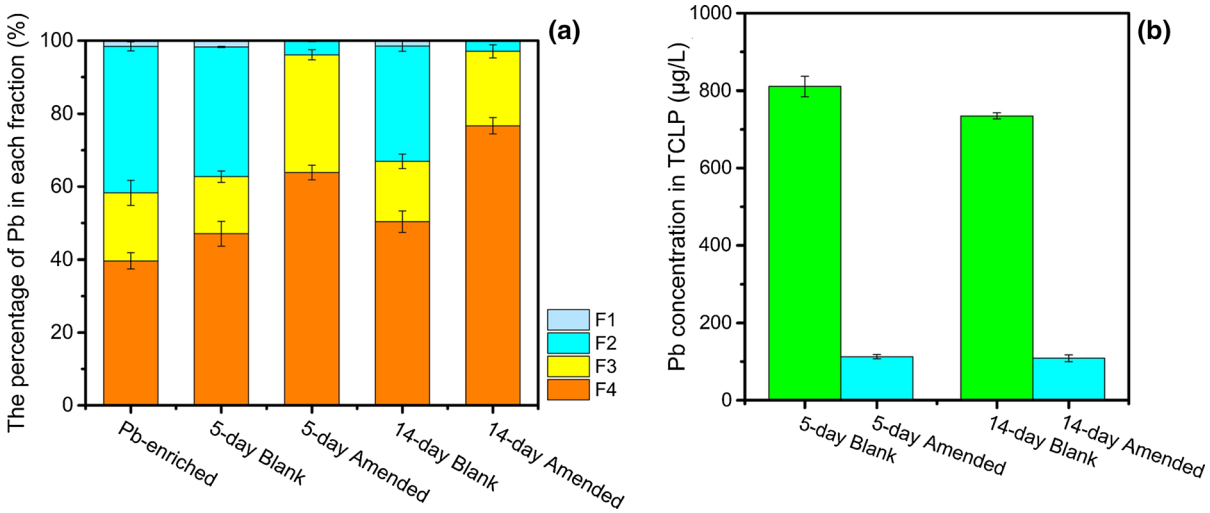

Fig. 4 **a** Weight percentages of different fractions (F1–F4) for Pb species, and **b** the concentration of Pb in leachates of blank and OSP-amended sediments. Pb-enriched means the sediments without incubation. "5-day Blank" and "14-day Blank" refer to the Pb-enriched sediments without any amendment incubated for 5 and 14 days. "5-day Amended" and "14-day Amended" mean the Pb-enriched sediment amended by OSP for 5 and 14 days incubation, respectively

leachates was found as 810.7 μg/L and 112.8 μg/L, respectively. Meanwhile, after 14 days incubation, the Pb concentration in the leachates was changed, respectively, to 734.9 μg/L and 108.6 μg/L for blank and amended samples. Therefore, it can be obviously found that the leachability of Pb has been declined substantially by around 7.0 times when the sediment was amended by the OSP either for 5 or 14 days. Moreover, when the Pb concentration was compared in leachates of amended sediments after 5 and 14 days, it can be observed that the leachability of Pb is quite similar to each other. The result indicates that a 5-day incubation is already effective for Pb stabilization but a prolonged incubation time can further enhance the change of Pb speciation from F3 to F4 as shown in Fig. 4a.

One previous study has applied the oyster shell for soil remediation (Ok et al. 2010), and the use of OSP for sediment remediation exhibited more favorable results for heavy metal stabilization in the sediments. With abundant water content in the sediment, the carbonates in the OSP can be dissolved and promote the ion change process. Moreover, the dissolved carbonates can also provide alkalinity, which further inhibit the conversion of metals from fixed states to mobile phases. Therefore, mechanisms for Pb stabilization by the OSP addition in the sediment can be either caused by the transformation of Pb into $PbCO_3$ and the potential precipitation caused by increased pH of the reaction system (Ok et al. 2011b).

Conclusion

In this study, the oyster shell powder (OSP) after simple pretreatment was adopted as a type of biogenic material for Pb(II) adsorption from the aquatic system and further for Pb(II) stabilization in the contaminated sediment. Characterization results showed the layer structure of OSP, with calcium carbonate (calcite) as the predominant component. The Pb(II) adsorption capacity of the OSP was up to 639.9 mg/g, indicating that the adsorption performance of OSP is excellent, especially when compared with the reported value from other studies. Ion exchange was regarded as the major mechanism for Pb(II) removal, which can be further verified from the Ca(II) concentration in solution after Pb(II) adsorption and the high peak intensities of the $PbCO_3$ on the surface of Pb-adsorbed OSP. Furthermore, the OSP was applied as the amendment for Pb(II) stabilization in the artificial contaminated river sediment. Results showed that percentage of F4 was increased substantially from 39.6% to 76.7% after 14 days incubation. Besides, the leachability of Pb has also been decreased by around 7.0 times when the sediment was amended by the OSP

even incubated by 5 days. Therefore, this study proposed the oyster shell as a cost-efficient and environmentally friendly biogenic material for effective metal immobilization, which can both recover the waste resources and further enhance the performance of sediment remediation. Moreover, with good performance for metal adsorption in aquatic environment together with the metal stabilization in sediment, it is possible that the OSP will be practically applied for the remediation of real river systems.

Acknowledgements This work is supported financially by the National Natural Science Foundation of China (NSFC) (41977329; 21707063) and the Science and Technology Innovation Committee of Shenzhen Municipality (JCYJ20160429191618506). This work is also sponsored by the Guangdong Provincial Key Laboratory of Soil and Groundwater Pollution Control (No. 2017B030301012) and the State Environmental Protection Key Laboratory of Integrated Surface Water-Groundwater Pollution Control.

Compliance with ethical standards

Ethical approval This work does not contain any studies with animals performed by any of the authors.

References

Alvarenga, R. A. F. D., Galindro, B. M., Helpa, C. D. F., & Soares, S. R. (2012). The recycling of oyster shells: An environmental analysis using life cycle assessment. *Journal of Environmental Management, 106,* 102–109. https://doi.org/10.1016/j.jenvman.2012.04.017

Audry, S., Schäfer, J., Blanc, G., & Jouanneau, J. M. (2004). Fifty-year sedimentary record of heavy metal pollution (Cd, Zn, Cu, Pb) in the lot river reservoirs (France). *Environmental Pollution, 132*(3), 413–426. https://doi.org/10.1016/j.envpol.2004.05.025

Basu, M., Guha, A. K., & Ray, L. (2017). Adsorption of lead on cucumber peel. *Journal of Cleaner Production, 151,* 603–615. https://doi.org/10.1016/j.jclepro.2017.03.028

Bozbaş, S. K., & Boz, Y. (2016). Low-cost biosorbent: Anadara inaequivalvis shells for removal of Pb(II) and Cu(II) from aqueous solution. *Process Safety and Environmental Protection, 103,* 144–152. https://doi.org/10.1016/j.psep.2016.07.007

Cerbo, A. A. V., Ballesteros, F., Chen, T. C., & Lu, M. C. (2017). Solidification/stabilization of fly ash from city refuse incinerator facility and heavy metal sludge with cement additives. *Environmental Science and Pollution Research, 24*(2), 1748–1756. https://doi.org/10.1007/s11356-016-7943-z

Che, Y., He, Q., & Lin, W. Q. (2003). The distributions of particulate heavy metals and its indication to the transfer of sediments in the Changjiang Estuary and Hangzhou Bay, China. *Marine Pollution Bulletin, 46*(1), 123–131. https://doi.org/10.1016/s0025-326x(02)00355-7

Dai, L., Wang, L., Li, L., Liang, T., Zhang, Y., Ma, C., et al. (2018). Multivariate geostatistical analysis and source identification of heavy metals in the sediment of Poyang Lake in China. *Science of the Total Environment, 621,* 1433–1444. https://doi.org/10.1016/j.scitotenv.2017.10.085

Du, Y., Lian, F., & Zhu, L. (2011). Biosorption of divalent Pb, Cd and Zn on aragonite and calcite mollusk shells. *Environmental Pollution, 159*(7), 1763–1768. https://doi.org/10.1016/j.envpol.2011.04.017

Fonti, V., Beolchini, F., Rocchetti, L., & Dell'Anno, A. (2015). Bioremediation of contaminated marine sediments can enhance metal mobility due to changes of bacterial diversity. *Water Research, 68,* 637–650. https://doi.org/10.1016/j.watres.2014.10.035

Guru, P. S., & Dash, S. (2014). Sorption on eggshell waste—A review on ultrastructure, biomineralization and other applications. *Advances in Colloid and Interface Science, 209,* 49–67. https://doi.org/10.1016/j.cis.2013.12.013

Hu, H., Zhang, Q., Yuan, W., Li, Z., Zhao, Y., & Gu, W. (2019). Efficient Pb removal through the formations of (basic) carbonate precipitates from different sources during wet stirred ball milling with $CaCO_3$. *Science of the Total Environment, 664,* 53–59. https://doi.org/10.1016/j.scitotenv.2019.01.424

Imamoglu, M., Şahin, H., Aydın, Ş, Tosunoğlu, F., Yılmaz, H., & Yıldız, S. Z. (2016). Investigation of Pb(II) adsorption on a novel activated carbon prepared from hazelnut husk by K_2CO_3 activation. *Desalination and Water Treatment, 57*(10), 4587–4596. https://doi.org/10.1080/19443994.2014.995135

Ip, C. C. M., Li, X. D., Zhang, G., Wai, O. W. H., & Li, Y. S. (2007). Trace metal distribution in sediments of the pearl river estuary and the surrounding coastal area, South China. *Enviromental Pollution, 147*(2), 311–323. https://doi.org/10.1016/j.envpol.2006.06.028

Islam, M. S., Choi, W. S., Nam, B., Yoon, C., & Lee, H. J. (2017a). Needle-like iron oxide@$CaCO_3$ adsorbents for ultrafast removal of anionic and cationic heavy metal ions. *Chemical Engineering, 307,* 208–219. https://doi.org/10.1016/j.cej.2016.08.079

Islam, M. N., Taki, G., Nguyen, X. P., Jo, Y. T., Kim, J., & Park, J. H. (2017b). Heavy metal stabilization in contaminated soil by treatment with calcined cockle shell. *Environmental Science and Pollution Research*, *24*, 7177–7183. https://doi.org/10.1007/s11356-016-8330-5

Jacob, J. J., Varalakshmi, R., Gargi, S., Jayasri, M. A., & Suthindhiran, K. (2018). Removal of Cr (III) and Ni (II) from tannery effluent using calcium carbonate coated bacterial magnetosomes. *NPJ Clean Water, 1*(1), 1. https://doi.org/10.1038/s41545-018-0001-2

Jung, S., Heo, N. S., Kim, E. J., Oh, S. Y., Lee, H. U., Kim, I. T., et al. (2016). Feasibility test of waste oyster shell powder for water treatment. *Process Safety and Environmental Protection, 102,* 129–139. https://doi.org/10.1016/j.psep.2016.03.004

Köhler, S. J., Cubillas, P., Rodríguez-Blanco, J. D., Bauer, C., & Prieto, M. (2007). Removal of cadmium from wastewaters by aragonite shells and the influence of other divalent

cations. *Environmental Scicence & Technology, 41*(1), 112–118. https://doi.org/10.1021/es060756j

Lee, M. E., Park, J. H., & Chung, J. W. (2019). Comparison of the lead and copper adsorption capacities of plant source materials and their biochars. *Journal of Environmental Management, 236,* 118–124. https://doi.org/10.1016/j.jenvman.2019.01.100

Liao, D., Zheng, W., Li, X., Yang, Q., Yue, X., Guo, L., et al. (2010). Removal of lead(II) from aqueous solutions using carbonate hydroxyapatite extracted from eggshell waste. *Journal of Hazardous Materials, 177*(1–3), 126–130. https://doi.org/10.1016/j.jhazmat.2009.12.005

Lim, A. P., Zulkeflee, Z., & Aris, A. Z. (2016). Effective removal of lead (II) ions by dead calcareous skeletons: Sorption performance and influencing factors. *Water Science and Technology, 74*(7), 1577–1584. https://doi.org/10.2166/wst.2016.368

Liu, Y., Tang, Y., Wang, P., & Zeng, H. (2019a). Carbonaceous halloysite nanotubes for the stabilization of Co, Ni, Cu and Zn in river sediments. *Environmental Science: Nano, 6*(8), 2420–2428.

Liu, Y., Tang, Y., Zhong, G., & Zeng, H. (2019b). A comparison study on heavy metal/metalloid stabilization in Maozhou river sediment by five types of amendments. *Journal of Soils and Sediments, 19,* 3922–3933. https://doi.org/10.1007/s11368-019-02310-w

Melichová, Z., & Ľuptáková, A. (2016). Removing lead from aqueous solutions using different low-cost abundant adsorbents. *Desalination and Water Treatment, 57*(11), 5025–5034. https://doi.org/10.1080/19443994.2014.999713

Moon, D. H., Cheong, K. H., Khim, J., Grubb, D. G., & Ko, I. (2011). Stabilization of Cu-contaminated army firing range soils using waste oyster shells. *Environmental Geochemistry and Health, 33*(S1), 159–166. https://doi.org/10.1007/s10653-010-9358-y

Ok, Y. S., Lee, S. S., Jeon, W.-T., Oh, S.-E., Usman, A. R. A., & Moon, D. H. (2011a). Application of eggshell waste for the immobilization of cadmium and lead in a contaminated soil. *Environmental Geochemistry and Health, 33*(S1), 31–39. https://doi.org/10.1007/s10653-010-9362-2

Ok, Y. S., Lim, J. E., & Moon, D. H. (2011b). Stabilization of Pb and Cd contaminated soils and soil quality improvements using waste oyster shells. *Environmental Geochemistry and Health, 33*(1), 83–91. https://doi.org/10.1007/s10653-010-9329-3

Ok, Y. S., Oh, S.-E., Ahmad, M., Hyun, S., Kim, K.-R., Moon, D. H., et al. (2010). Effects of natural and calcined oyster shells on Cd and Pb immobilization in contaminated soils. *Environmental Earth Sciences, 61*(6), 1301–1308. https://doi.org/10.1007/s12665-010-0674-4

Peng, W., Li, X., Xiao, S., & Fan, W. (2018). Review of remediation technologies for sediments contaminated by heavy metals. *Journal of Soils and Sediments, 18*(4), 1701–1719. https://doi.org/10.1007/s11368-018-1921-7

Rađenović, D., Kerkez, Đ, Pilipović, D. T., Dubovina, M., Grba, N., Krčmar, D., et al. (2019). Long-term application of stabilization/solidification technique on highly contaminated sediments with environment risk assessment. *Science of the Total Environment, 684,* 186–195. https://doi.org/10.1016/j.scitotenv.2019.05.351

Wang, L., Chen, L., Cho, D.-W., Tsang, D. C. W., Yang, J., Hou, D., et al. (2019). Novel synergy of Si-rich minerals and reactive MgO for stabilisation/solidification of contaminated sediment. *Journal of Hazardous Materials, 365,* 695–706. https://doi.org/10.1016/j.jhazmat.2018.11.067

Wu, Q., Chen, J., Clark, M., & Yu, Y. (2014). Adsorption of copper to different biogenic oyster shell structures. *Applied Surface Science, 311,* 264–272. https://doi.org/10.1016/j.apsusc.2014.05.054

Xia, W.-Y., Feng, Y.-S., Jin, F., Zhang, L.-M., & Du, Y.-J. (2017). Stabilization and solidification of a heavy metal contaminated site soil using a hydroxyapatite based binder. *Construction and Building Materials, 156,* 199–207. https://doi.org/10.1016/j.conbuildmat.2017.08.149

Zhang, M., Wang, X., Yang, L., & Chu, Y. (2019a). Research on progress in combined remediation technologies of heavy metal polluted sediment. *International Journal of Environmental Research and Public Health, 16*(24), 5098. https://doi.org/10.3390/ijerph16245098

Zhang, Z., Chen, H., Guo, G., & Li, F. (2019b). Amendments for simultaneous stabilization of lead, zinc, and cadmium in smelter-contaminated topsoils. *Environmental Engineering Science, 36*(3), 326–334. https://doi.org/10.1089/ees.2018.0231

Zhou, Q., Liao, B., Lin, L., Qiu, W., & Song, Z. (2018). Adsorption of Cu(II) and Cd(II) from aqueous solutions by ferromanganese binary oxide–biochar composites. *Science of the Total Environment, 615,* 115–122. https://doi.org/10.1016/j.scitotenv.2017.09.220